A single nonpolar residue in the deep pore of related K^+ channels acts as a K^+:Rb^+ conductance switch

G. E. Kirsch,* ‡ J. A. Drewe,* M. Taglialatela,* R. H. Joho,* Mariella DeBiasi,* H. A. Hartmann,* and A. M. Brown*

*Department of Molecular Physiology and Biophysics, ‡Department of Anesthesiology, Baylor College of Medicine, Houston, Texas 77030 USA

ABSTRACT K^+ and Rb^+ conductances (G_{K^+} and G_{Rb^+}) were investigated in two delayed rectifier K^+ channels (Kv2.1 and Kv3.1) cloned from rat brain and a chimera (CHM) of the two channels formed by replacing the putative pore region of Kv2.1 with that of Kv3.1. CHM displayed ion conduction properties which resembled Kv3.1. In CHM, G_{K^+} was three times greater than that of Kv2.1 and $G_{Rb^+}/G_{K^+} = 0.3$ (compared with 1.5 and 0.7, respectively, in Kv2.1 and Kv3.1). A point mutation in CHM L374V, which restored 374 to its Kv2.1 identity, switched the K^+/Rb^+ conductance profiles so that G_{K^+} was reduced fourfold, G_{Rb^+} was increased twofold, and $G_{Rb^+}/G_{K^+} = 2.8$. Quantitative restoration of the Kv2.1 K^+/Rb^+ profiles, however, required simultaneous point mutations at three nonadjacent residues suggesting the possibility of interactions between residues within the pore. The importance of leucine at position 374 was verified when reciprocal changes in K^+/Rb^+ conductances were produced by the mutation of V374L in Kv2.1 (G_{K^+} was increased threefold, G_{Rb^+} was decreased threefold, and $G_{Rb^+}/G_{K^+} = 0.2$). We conclude that position 374 is responsible for differences in G_{K^+} and G_{Rb^+} between Kv2.1 and Kv3.1 and, given its location near residues critical for block by internal tetraethylammonium, may be part of a cation binding site deep within the pore.

INTRODUCTION

The ion conduction pore of voltage-sensitive K^+ channels has been interpreted by mutational analysis to lie in the highly conserved loop connecting membrane-spanning α-helices S5 and S6 of the consensus topographical channel model (Tempel et al., 1988; Baumann et al., 1988). Single point mutations in this loop have identified critical amino acids controlling sensitivity to the pore blockers charybdotoxin (MacKinnon and Miller, 1989; MacKinnon et al., 1990), tetraethylammonium (TEA) (MacKinnon and Yellen, 1990; Yellen et al., 1991), and modulating ion selectivity (Yool and Schwarz, 1991). In the absence of structural information the interpretation is weakened by the possibility that the changes produced by single mutations could have been due to remote effects. To avoid this limitation, a chimeric approach was taken having as its goal the transfer of a set of distinctive pore properties between two related K^+ channels. To this end, a 25 amino acid segment (Fig. 1, amino acid residues 364–388) that included the critical residues for internal TEA blockade (Yellen et al., 1991) and ion selectivity (Yool and Schwarz, 1991) was transplanted from a donor K^+ channel to a recipient K^+ channel, the two channels differing from each other in K^+ conductance and TEA blockade (Hartmann et al., 1991). The transplanted segment completely transferred this donor phenotype to the host channel (Hartmann et al., 1991). The result suggested that ion conduction properties were specified entirely by the donor peptide module without modification by the host channel. As a further test of this hypothesis, we expanded the scope of our analysis by probing the pore with the K^+ analogue, Rb^+. These two ions have crystal radii of 1.33 and 1.48 Å, respectively (Hille, 1984), and might reveal otherwise unsuspected structural changes in the putative pore. In addition, the differences in amino acids within the pore segment were exploited in order to establish which residues determined the phenotypic differences.

Conduction of K^+ and Rb^+ was investigated in two delayed rectifier K^+ channels cloned from rat brain, Kv2.1 (using simplified nomenclature recently introduced by Chandy [1991] and formerly DRK1; Frech et al., 1989) and Kv3.1 (formerly NGK2; Yokoyama et al., 1989), and in a chimera of the two channels here called CHM, described by Hartmann et al. (1991). To form the chimera, a segment was transplanted that extended between positions 364 and 388 of the host K^+ channel. The residues exchanged at positions 364–368 were identical so that the effective exchange involved 21 residues. Of these 21 residues only 9 were not identical and could have produced the functional differences between Kv2.1 and Kv3.1 and it is on these residues that the present experiments were focused.

Address correspondence to Dr. A. M. Brown.

0006-3495/92/04/136/09 $2.00

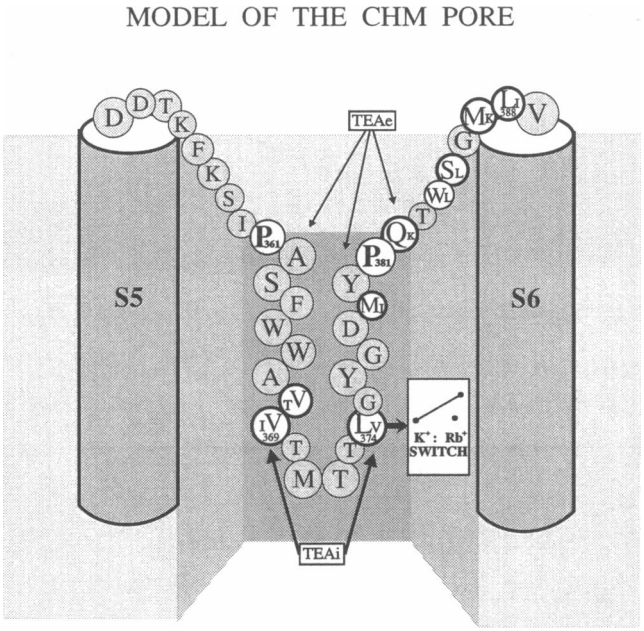

FIGURE 1 Diagram of the CHM pore. The residues comprise the loop between transmembrane segments 5 and 6. Two highlighted prolines at positions 361 and 381 set the bounds for membrane entry and exit of a β-sheet composed of two antiparallel β-strands. This region is referred to as the deep pore. Nine residues other than the prolines are highlighted and differ between the donor Kv3.1 channel and the host Kv2.1 channel, with the Kv3.1 residues in larger type. Assuming a K^+ channel homotetramer with fourfold symmetry, four β-sheets would form a β-barrel. The residues that align with Shaker residues influencing blockade by charybdotoxin (CTX) and TEA are indicated by arrows. Also indicated are the pair of deep pore residues (369 and 374) that determine the differences in pore phenotypes between Kv2.1 and Kv3.1. Single letter amino acid code was: A, Ala; R, Arg; D, Asp; N, Asn; C, Cys; Q, Gln; E, Glu; G, Gly; I, Ile; L, Leu; K, Lys; M, Met; F, Phe; P, Pro; S, Ser; T, Thr; Y, Tyr; W, Trp; V, Val; H, His.

METHODS

Standard recombinant DNA techniques

Standard methods of plasmid DNA preparation, site-directed mutagenesis and DNA sequencing were used (Sambrook et al., 1989). The parent clone Kv2.1 (Frech et al., 1989), Kv3.1 (Yokoyama et al., 1989) and the chimeric clone CHM (Hartmann et al., 1991), as well as the site-directed mutants of the clones, were propagated in the transcription-competent plasmid vector pBluescript SK(−) in the Xl1-blue *E. coli* strain (Stratagene, La Jolla, CA).

Site-directed mutagenesis of CHM

To obtain a single stranded DNA template for specific oligodirected mutagenesis, CHM or Kv2.1 was first digested with BamHI (+909 and +1,520). The resultant 611 nucleotide fragment was subcloned into BamHI digested M13mp19 single stranded phagemid. Mutagenesis was performed using an Amersham kit (Life Sciences, Arlington Heights, IL) as described previously (Moorman et al., 1990). Briefly, complementary oligonucleotides, 24–29 bases in length, were synthesized (Applied Biosystems, Foster City, CA) with one to three base mutants for each of the constructs in CHM: V368T, V369I, L374V, M379I, Q382K, W384L, S385L, M387K, and L388I; and for Kv2.1 V374L. A combined oligonucleotide was synthesized for CHM A362I + S363G. The mutated restriction fragment was cloned back into the original BamHI cut CHM or Kv2.1. Double or triple mutations were done using templates that already contained single or double mutations, respectively. The region spanning the BamHI sites was then verified by sequencing.

In vitro transcription and oocyte injection

Preparation of cRNA and oocyte injection utilizing T7 RNA polymerase and in vitro capping (Joho et al., 1990) have been described previously. Stage V or VI oocytes were injected with 75 nl of cRNA solutions, 10–200 pg/nl, and tested for the expression of functional K^+ channels 3–4 d after injection. Before electrophysiological recordings were performed, the follicular layer of cells was removed manually from the oocytes. For patch recordings, the vitelline layer was removed manually.

Electrophysiology

Patch clamp recording

Oocytes were placed in a recording chamber containing isotonic KCl depolarizing solution. Single channel recordings were obtained from cell-attached and inside-out membrane patches using fire-polished, Sylgard-coated (Dow-Corning, Midland, MI) micropipettes of 2–5 MΩ resistance. Holding and test potentials applied to the membrane patch were reported as conventional absolute intracellular potentials assuming that the oocyte resting potential was zeroed by the bathing solution. Experiments were performed at room temperature (21–23°C).

Patch pipettes were filled with normal frog Ringers solution which consisted of (in millimolar): 120 NaCl, 2.5 KCl, 2 $CaCl_2$, 10 Hepes, pH 7.2 (adjusted with NaOH). In some experiments NaCl + KCl was replaced with either KCl or RbCl at 122.5 mM. Depolarizing bath solution consisted (in millimolar): 100 KCl, 6 EGTA, 10 Hepes, pH 7.2 (adjusted with KOH). In some experiments RbCl and RbOH, respectively, replaced KCl and KOH. Bathing solution flowed continuously at a rate of 1 ml/min.

Data were low-pass filtered at 2 kHz. (−3 dB, 4-pole Bessel filter) before digitization at 10 kHz. Channels were activated with rectangular test pulses from negative holding potentials or with voltage ramps from +100 to −100 mV (at either 5 or 1 mV/ms). In the figures, the start of the current trace coincides with the start of the stimulus. Holding potentials were adjusted to minimize simultaneous openings of multiple channels.

Pulse-stimulated currents were analyzed as follows. Records were corrected for linear capacitative and leakage current by subtracting the smoothed average of records lacking channel activity (null traces) and low-pass filtered at 0.5–1 kHz. Transitions between closed and open levels were detected using a threshold set at one-half the amplitude of the unitary current. Computer-detected openings were collected into amplitude and open time distribution histograms. Amplitude histograms were fit by Gaussian functions using a maximum likelihood estimate. Open events of <1.8 ms duration were excluded from the histogram to avoid errors arising from bandwidth limitations.

Ramp-stimulated currents were analyzed by first subtracting capacitative and leakage currents using null traces as above. Traces containing single channel openings were selected and segments containing closed intervals or overlapping openings of multiple channels were set to zero. The remaining nonzero points were averaged to give a continuous open channel current-voltage (I-V) relationship. Each I-V curve contains data from 12 to 16 ramps.

Whole-cell recording

Defolliculated oocytes were impaled with two microelectrodes and voltage clamped using a commercial amplifier (Dagan 8500; Dagan Corp., Minneapolis, MN). Both the voltage-sensing and current-passing electrodes were filled with 3M KCl, 10 mM Hepes, pH 7.4 (1–2 MΩ resistance). Linear leakage and capacity currents were subtracted on-line using a P/4 pulse protocol. Membrane potentials were not corrected for series resistance error.

External bathing solution consisted (in millimolar) of either: 100 *N*-methyl-D-glucamine (NMDG), 100 MES, 2.5 KOH, 2 MgOH, and 10 Hepes, pH 7.4; or normal frog Ringers solution, as described above. In ion selectivity experiments NMDG-MES + K-MES was replaced with either KCl or RbCl at 100 mM. The oocytes were superfused with solution at 2 ml/min. The experiments were performed at room temperature (21–23°C).

RESULTS

As shown in Fig. 2, single channel ion conductance was characterized in symmetrical 120 mM KCl and RbCl solutions using voltage ramps from +100 to −100 mV. The I-V relationships in the three channel types could be distinguished by three features: (*a*) both CHM and Kv3.1 showed clear inward rectification in symmetrical K^+ solutions, whereas Kv2.1 was nearly linear; (*b*) the outward K^+ slope conductance (G_{K^+}) of both CHM and Kv3.1 was about three times greater than that of Kv2.1 and, because of the inward rectification, an even larger difference was observed for inward K^+ conductance; and (*c*) in Kv2.1 the Rb^+ conductance (G_{Rb^+}) profile overlapped the K^+ profile whereas for both CHM and Kv3.1, G_{Rb^+} was lower than G_{K^+} for both inward and outward currents. An important quantitative difference between CHM and Kv3.1 however, was that G_{Rb^+} was much lower in CHM than Kv3.1.

A plausible explanation for this difference is that the pore of the chimeric channel was distorted in a way that was not detected by K^+ but was apparent when Rb^+ was the conducting species. Alternatively, the 21 residues exchanged in the chimera did not include residues which regulate G_{Rb^+} in Kv3.1. For instance, position 363 lies within the putative pore and is just upstream from the exchanged segment which began at F364 (Fig. 1) but is a serine in CHM and a glycine in Kv3.1. The difference in side chain polarity might be expected to influence ion conduction, particularly if the side chain is exposed to the aqueous lumen of the pore.

To test this idea we mutated CHM to form CHM

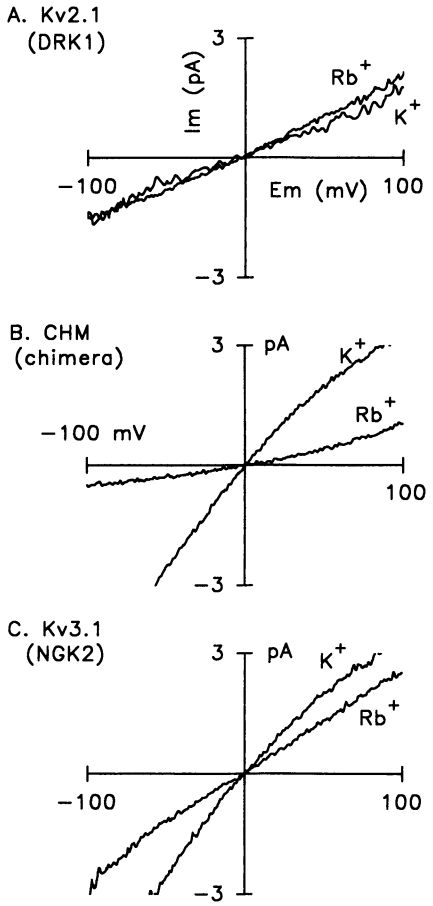

FIGURE 2 Comparison of K^+/Rb^+ I-V profiles in three K^+ channels. Single channel I-V curves were obtained in inside-out patches by applying a ramp stimulus from +100 to −100 mV. Records were low-pass filtered at 2 kHz. After subtraction of linear leakage and capacitative currents, segments of traces containing single channel openings were averaged. Each curve is the average of 16 traces from single patches exposed to 120 mM KCl or RbCl at both intra- and extracellular surfaces.

A362I + S363G, thus completely reproducing the Kv3.1 sequence in the β-hairpin between the two prolines (Fig. 1). As shown in Fig. 3, and Table 1, the new chimeric channel was indistinguishable from the original CHM. Under biionic conditions (internal K^+, external Rb^+), the outward K^+ limb of the I-V curve in both chimeric channels, as well as Kv3.1, superimposed, whereas inward currents carried by Rb^+ in the chimeric channels were indistinguishable from one another but were clearly less Rb^+ conductive than in Kv3.1 (Table 1). By considering the reversal potentials in this experiment we can compare the differences in P_{Rb^+}/P_{K^+} versus G_{Rb^+}/G_{K^+}. As shown in Fig. 3, reversal potentials of −13 and −10 mV, respectively, were obtained from CHM and Kv3.1. Assuming a reversal potential of zero mV in symmetrical

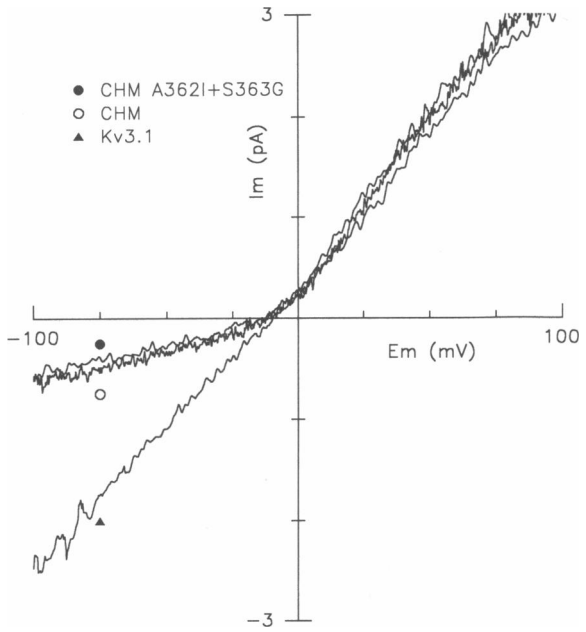

FIGURE 3 K^+/Rb^+ I-V relationships under biionic conditions. Single channel I-V ramps were obtained in inside-out patches exposed intracellularly to 120 KCl and extracellularly to 120 RbCl.

K^+ (Fig. 2) gave $P_{Rb}{}^+/P_K{}^+$ of 0.61 and 0.68, respectively, for CHM and Kv3.1. By contrast, a much greater degree of Rb^+/K^+ discrimination was evident in the $G_{Rb}{}^+/G_K{}^+$ ratios. The slope conductances obtained from the linear inward regions of the I-V plots in Figs. 2 and 3, for example, give $G_{Rb}{}^+/G_K{}^+$ ratios of 0.12 and 0.47, respectively, for CHM and Kv3.1. For both channels the greater degree of ion discrimination obtained from conductance versus permeability ratios suggests that Rb^+ is only slightly less permeant than K^+ but, in addition, binds within the pore resulting in a partial block. The markedly lower Rb^+ conductance of CHM compared to Kv3.1 is not reflected in reversal potential

TABLE 1 K^+/Rb^+ conductance under bi-ionic conditions compared between a chimeric K^+ channel and its dominant parent

Channel	$G_K{}^+$ out	$G_{Rb}{}^+$ in	E_{rev}
	pS	*pS*	*mV*
CHM	36.6 ± 1.2 (3)	5.0 ± 1.5 (3)	−17.0 ± 4.6 (3)
CHM A362I + S363G	32.3 ± 2.4 (4)	4.5 ± 1.3 (4)	−16.4 ± 1.9 (4)
Kv3.1	33.7 ± 2.0 (6)	25.0 ± 0.9 (6)	−14.0 ± 3.4 (6)

$G_{Rb}{}^+$ in, $G_K{}^+$ out = chord conductances measured for biionic ramp I-V data (e.g., Fig. 3 at voltages ±60 mV from the zero current potential. Mean ± SD (n = number of inside-out patches). External solution = 120 mM RbCl, internal solution = 120 mM KCl. E_{rev} = zero current potential obtained directly from single channel I-V curves.

measurements and suggests that Rb^+ binds with higher affinity to CHM than to Kv3.1.

Identification of single amino acid determinants of K^+/Rb^+ conductance

We next attempted to identify which residues might be critical for K^+/Rb^+ binding in the pore. Each of the nine amino acid differences between CHM and Kv2.1 was reverted back to its corresponding Kv2.1 identity by point mutations in CHM. The results are summarized in Table 2. Of the nine single point mutations only L374V affected K^+ conductance. Furthermore, as shown in Fig. 4, L374V had the remarkable effect of inverting the $G_{Rb}{}^+/G_K{}^+$ discrimination observed in CHM; instead of being blocked by Rb^+, CHM L374V appears to be blocked by K^+. Thus in Fig. 4 *C*, the slope conductance became nearly threefold greater for outward Rb^+ current than for K^+ current and, compared with the original CHM, $G_K{}^+$ was reduced fourfold (Table 2). By contrast, in tests of six of the other point reversions, $G_{Rb}{}^+/G_K{}^+$ was unchanged (Table 2). For the remaining two reversions in which $G_{Rb}{}^+$ was not measured, Q382K and L388I, no change in $G_K{}^+$ occurred and, given the reciprocal relationship between $G_{Rb}{}^+$ and $G_K{}^+$ in CHM and L374V channels, this suggests that $G_{Rb}{}^+$ was not altered. In addition, Q382K was unlikely to have had much effect on $G_{Rb}{}^+$ because in the double reversion, CHM L374V + Q382K, $G_{Rb}{}^+/G_K{}^+$, was the same as for CHM L374V (Table 2).

Whereas the $G_{Rb}{}^+/G_K{}^+$ was inverted for CHM L374V, Rb^+/K^+ selectivity was affected to a much smaller degree. Biionic reversal potential measurements were obtained using whole-cell, two microelectrode voltage clamp. Substitution of 100 mM RbCl for KCl shifted the reversal potential (in mV): −1.2 ± 1.4 (n = 4 cells), −11.7 ± 1.5 (3) and −3.8 ± 2.9 (5) in Kv2.1, CHM and CHM L374V, respectively. From these data we calculated (Hille, 1984) $P_{Rb}{}^+/P_K{}^+$ values of 1.0, 0.6, and 0.9 for Kv2.1, CHM and CHM L374V, respectively. Thus, in CHM the mutation L374V increased $G_{Rb}{}^+$ relative to $G_K{}^+$ by 800% whereas the Rb^+/K^+ selectivity ratio increased only 50%.

Position 374 as a determinant of K^+/Rb^+ conductance in the host Kv2.1 channel

To further assess the importance of position 374 for $G_{Rb}{}^+/G_K{}^+$ discrimination, we mutated V374L in Kv2.1 because CHM has an L at this position. As shown in Fig. 4 *D–F*, and as predicted from the results in CHM, this mutation strongly enhanced Rb^+ block and increased $G_K{}^+$ from 8.4 pS in the unmutated Kv2.1 channel to 23.6 pS, a value close to that of CHM (Table 2). In whole-cell

TABLE 2 K^+/Rb^+ conductance in a chimeric K^+ channel and its parent channels

Channel	G_{K^+}	G_{Rb^+}	G_{Rb^+}/G_{K^+}
	pS	*pS*	
Kv2.1	8.4 ± 1.2 (15)	12.8 ± 0.6 (4)	1.5
Kv3.1	23.2 ± 3.3 (11)	14.2 ± 2.5 (5)	0.7
Chimera (CHM)	21.5 ± 5.0 (11)	6.8 ± 1.4 (6)	0.3
CHM V368T	22.0 ± 2.4 (7)	6.9 ± 1.1 (5)	0.3
CHM V369I	36.9 ± 2.4 (4)*	7.1 ± 0.9 (3)	0.2
CHM L374V	5.3 ± 0.7 (5)	14.7 ± 0.5 (5)	2.8
CHM M379I	21.0 ± 0.7 (6)	3.9 ± 0.2 (2)	0.2
CHM Q382K	18.2 ± 0.9 (5)	nd	nd
CHM W384L	25.3 ± 1.4 (3)	6.0 ± 1.3 (7)	0.2
CHM S385L	21.4 ± 1.2 (4)	6.4 ± 1.3 (5)	0.3
CHM M387K	22.3 ± 0.7 (5)	4.4 ± 1.0 (3)	0.2
CHM L388I	25.6 ± 1.4 (3)	nd	nd
Kv2.1 V374L	23.6 ± 2.3 (9)	4.1 ± 1.4 (4)	0.2
CHM L374V + V368T	5.6 ± 0.8 (4)	16.9 ± 1.7 (3)	3.0
CHM L374V + V369I	10.2 ± 0.6 (9)	26.4 ± 2.0 (4)	2.6
CHM L374V + V379I	4.6 ± 0.4 (3)	17.0 ± 1.6 (3)	3.7
CHM L374V + Q382K	4.1 ± 0.2 (5)	15.1 ± 0.8 (4)	3.7
CHM L374V + V369I + V368T	8.2 ± 0.4 (4)	22.3 ± 1.6 (3)	2.7
CHM L374V + V369I + M379I	10.4 ± 1.1 (5)	21.5 ± 1.2 (4)	2.1
CHM L374V + V369I + Q382K	8.9 ± 0.8 (8)	15.5 ± 2.5 (5)	1.7

G_{K^+}, G_{Rb^+} = mean single channel outward slope conductance ±SD (n = number of patches) measured in cell-attached (open cell) and inside-out patches with intracellular solutions containing either 120 mM K^+ or 120 mM Rb^+. Open cell means that the fluid in the bath exchanged completely with that in the cytoplasm so that the patches were effectively the same as inside-out patches. Extracellular solution was Na^+ Ringer except as noted below. *Data obtained in 120 mM external K^+. Average G_{K^+} for Kv2.1 and CHM in K^+ Ringer was 14.0 and 34.6 pS, respectively. All other data obtained in normal Na^+ Ringer. External Na^+ neither blocks nor conducts in these channels. nd = not determined.

voltage clamp, substitution of 100 mM external RbCl for KCl shifted the reversal potential −16.1 ± 3.2 mV (n = 5 cells), corresponding to a P_{Rb^+}/P_{K^+} = 0.54, comparable to 0.64 in CHM.

Initially we expected the same degree of block by Rb^+ in all three channels where position 374 contains a leucine (CHM, Kv2.1 V374L, and Kv3.1). However, as shown in Fig. 4 *G–I* and Table 2, Rb^+ conductance was much greater in Kv3.1 than in either CHM or Kv2.1 V374L when measured under the same conditions. These results suggest that if residue 374 is part of the lining of the pore, its side chain may interact with the rest of the channel protein.

Restoration of host K^+/Rb^+ conductance in the chimeric channel

As shown in Fig. 5 *A* and *D*, the symmetrical K^+ and Rb^+ profiles of CHM L374V were exaggerated versions of Kv2.1 in the sense that G_{K^+} undershot and G_{Rb^+} overshot Kv2.1. This result suggested the possibility that residues within the pore might interact. We then tried to determine which additional reversions were necessary to completely restore the K^+ and Rb^+ profiles of CHM L374V to those of Kv2.1. As summarized in Table 2, four other candidate point reversions were paired with L374V but only V369I increased G_{K^+} to a level comparable to Kv2.1. As shown in Fig. 5 *B* and Table 2, the K^+ profile of CHM L374V + V369I was similar to Kv2.1, but as indicated in Fig. 5 *C* and *F*, a near perfect superposition for both symmetric K^+ and Rb^+ profiles was achieved in the triple mutant CHM L374V + V369I + Q382K.

DISCUSSION

In our model of the pore (Fig. 1), the membrane is spanned by a β-hairpin between two proline residues located at positions 361 and 381. In this way the model can accommodate those residues responsible for block at the external mouth by charybdotoxin and TEA and block at the internal mouth by TEA (Yellen et al., 1991) because the extended conformation of a β-strand would permit nine residues to traverse the 30 Å thickness of the membrane. Assuming a homotetrameric channel (MacKinnon, 1991) with fourfold symmetry, the pore would be formed by a β-barrel. Turns in β-barrels usually form active sites (Wilson et al., 1981) and position 374 is at the COOH-terminus end of the hairpin turn. This is consistent with the importance of position

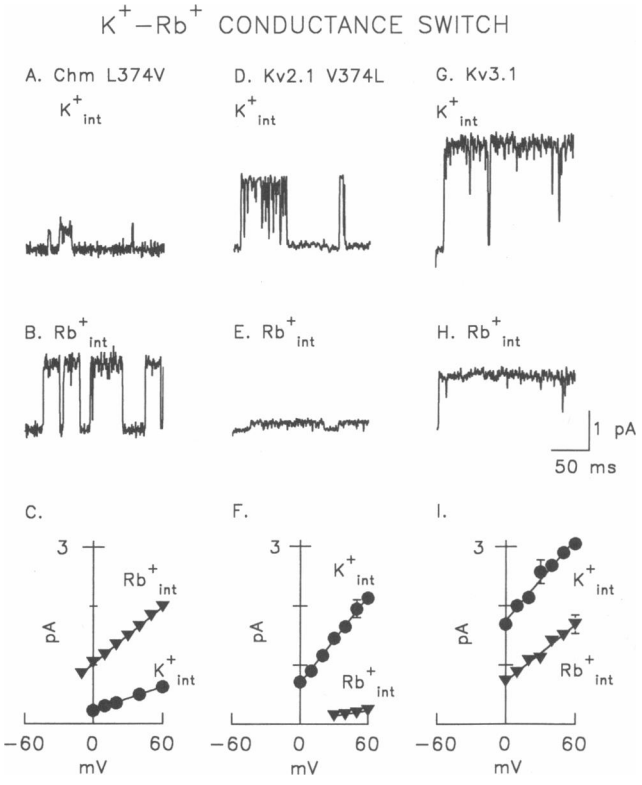

FIGURE 4 Identification of a critical residue for controlling K^+-Rb^+ conductance switching. Single channel records were obtained in inside-out patches exposed extracellularly (pipette solution) to normal 120 mM Na^+ Ringers solution and intracellularly to either 120 KCl (*A*, *D*, *G*) or 120 RbCl (*B*, *E*, *H*) solutions. Test potential was 40 mV. The level of resting inactivation was adjusted by varying the holding potential between −120 to −60 mV to facilitate recording single channel activity in multi-channel patches. Test pulse duration was 185 ms. Records were low-pass filtered at 500 Hz. Current-voltage (I-V) relationships (*C*, *F*, *I*) were determined at test potentials between −10 and +60 mV. The average single channel amplitudes obtained from amplitude histograms are plotted versus test potential. The data points are mean values obtained from 4 to 12 patches. Slope conductances were determined from least squares fits of the I-V data.

374 as a determinant of ion conduction in the pore and the relative K^+/Rb^+ conductance in CHM and in Kv2.1 as well. In the model, position 369 is across from 374 at the NH_2-terminus of the turn and the two might be interacting. However, we cannot exclude additive energetic contributions from these two residues which are dominants for pore function. Energetic interactions between two distant residues has been clearly shown in double mutation experiments that defined the active site of tyrosyl-tRNA synthetase (Carter et al., 1984).

Despite its importance as a determinant of G_{Rb^+}/G_{K^+}, the same leucine at position 374 was associated with different Rb^+ conductances in Kv2.1, Kv3.1, and CHM, suggesting that the side chain projected away from the pore. Further support for this was the observation that mean open time for CHM L374V was shortened fivefold (Kirsch et al., 1992) because this result would be consistent with the idea that the side chain at this position contacts other parts of the protein. Kinetic changes were prominent for the CHM V369I reversion consistent with an outward projection of the side chain at position 369. If the side chains at these positions do face outward then for single filing in this region permeant cations must be coordinated by a peptide backbone carbonyls. Cation coordination by a peptide backbone is widely accepted for the β-helix of the gramicidin A channel (Andersen, 1984) and interactions of the nonpolar side chains at position 374 with other residues might distort the pore geometry. An additional possibility is that the large changes in Rb^+ conductance may be related to interactions that change the flexibility of the peptide backbone of the pore (Roux and Karplus, 1991). Rb^+ by virtue of its larger radius may be more sensitive than K^+ to changes in pore flexibility.

The difference in inward Rb^+ current between CHM and Kv3.1 persisted even after the corrections at positions 362 and 363. This may reflect distortion or altered flexibility of the chimeric pore. Distortion could also explain the large effect on Rb^+ current of the reversion at position 382 when it was combined with the double reversions at positions 369 and 374 (Fig. 5). For K^+ currents, the double reversions restored most of the host K^+ conductance profile (Fig. 5) and the internal TEA blockade while the reversion at position 382 had as its main effect restoration of external TEA blockade (Kirsch et al., 1992).

The changes in Rb^+/K^+ conductance differ from those reported by Yool and Schwarz (1991) in Shaker K^+ channels. For their single point mutations, K^+ conductance remained unaltered although large changes in NH_4^+ and smaller changes in Rb^+ conductance. This was interpreted to indicate separate binding sites for K^+ and the other two ions. In our experiments a single point mutation changed both Rb^+ and K^+ conductance in a reciprocal fashion, consistent with a single ion-selective site.

In terms of the information they provide about structural details, our results certainly may have other interpretations. An α-helix of nine residues which could not by itself span the membrane, might only need to span part of the membrane if it were the inner layer of concentric layers of longer α-helices (Lodish, 1988). Even if a β-barrel were present, the side chains at positions 374 and 369 need not point outward because differences at these positions could change the appearance of the peptide backbone encountered by permeant cations. However, there can be very little doubt that a substantial part of the pore of K^+ channels has been localized within the linear sequence of these proteins. A specific double mutation in the transplanted segment of

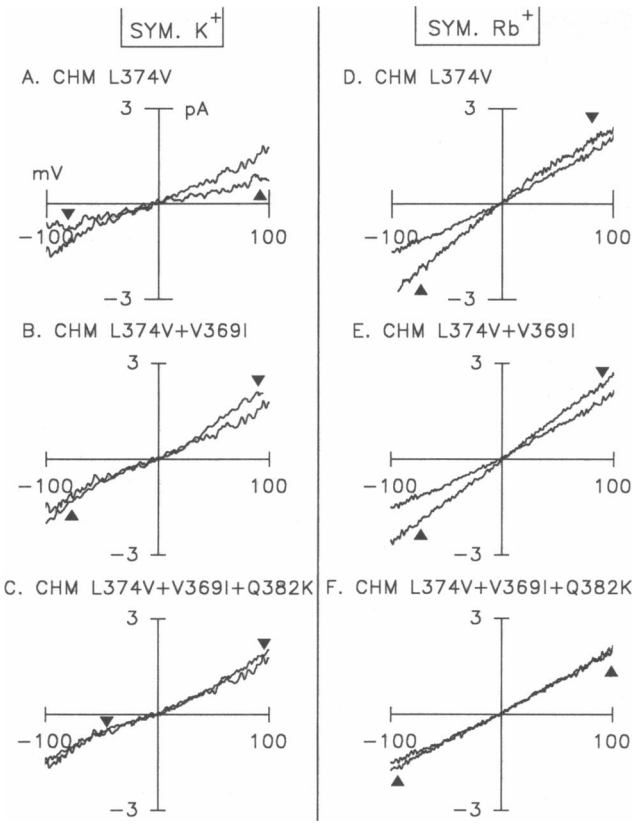

FIGURE 5 Interactions among residues modulate K^+/Rb^+ I-V profiles in CHM reversion mutants. Single channel I-V ramps were obtained in inside-out patches exposed at the intracellular surface to either symmetric 120 KCl (*A–C*) or symmetric 120 RbCl (*D–F*). In each graph the CHM reversion mutant data (marked by the two *arrowheads*) is superimposed over reference data from Kv2.1.

the chimeric channel restored most of the K^+ and Rb^+ conductance of the host channel as well as the profile of TEA blockade; a specific triple mutation restored the entire phenotype as we have measured it. Because of their conservative nature, the differences at positions 369 and 374 would ordinarily not have been prime candidates for single point mutations. The great advantage of chimeric constructs is that they provide direct clues, both about the residues to be mutated and the mutations to be made. Such constructs are based on the reasonable assumption that large proteins such as ion channels have their multiple functions performed by separable domains.

We thank M. Champagne and K. Davis for help with mutagenesis, G. Schuster and W. Dong for help with oocyte injections, and J. Breedlove for her secretarial assistance.

This work was supported in part by National Institutes of Health grants NS23877 (to A. M. Brown), NS29473 (to G. E. Kirsch) NS08805 (to J. A. Drewe), NS28407 to R. H. Joho, and a grant from the Italian National Research Council (CNR) to M. Taglialatela.

REFERENCES

Andersen, O. S. 1984. Gramicidin channels. *Annu. Rev. Physiol.* 46:531–548.

Baumann, A., A. Grupe, A. Ackermann, and O. Pongs. 1988. Structure of the voltage-dependent potassium channel is highly conserved from Drosophila to vertebrate central nervous system. *EMBO (Eur. Mol. Biol. Organ.) J.* 7:2457–2463.

Carter, P. J., G. Winter, A. J. Wilkinson, and A. R. Fersht. 1984. The use of double mutants to detect structural changes in the active site of the Tyrosyl-tRNA synthetase (*Bacillus stearothermophilus*). *Cell.* 38:835–840.

Chandy, K. G. 1991. Simplified gene nomenclature. *Nature (Lond.).* 352:26.

Frech, G. C., A. M. J. VanDongen, G. Schuster, A. M. Brown, and R. H. Joho. 1989. A novel potassium channel with delayed rectifier properties isolated from rat brain by expression cloning. *Nature (Lond.).* 340:642–645.

Hartmann, H. A., G. E. Kirsch, J. A. Drewe, M. Taglialatela, R. H. Joho, and A. M. Brown. 1991. Exchange of conduction pathways between two related K^+ channels. *Science (Wash. DC).* 251:942–944.

Hille, B. 1984. Ion channels of excitable membranes. Sinauer Associates. Sunderland, MA. 184–188.

Iverson, L. E., M. A. Tanouye, H. A. Lester, N. Davidson, and B. Rudy. 1988. A-type potassium channels expressed from Shaker locus cDNA. *Proc. Natl. Acad. Sci. USA.* 85:5723–5727.

Joho, R. H., J. R. Moorman, A. M. J. VanDongen, G. E. Kirsch, H. Silberberg, G. Schuster, and A. M. Brown. 1990. Toxin and kinetic profile of rat brain type III sodium channels expressed in Xenopus oocytes. *Mol. Brain Res.* 7:105–113.

Kirsch G. E., J. A. Drewe, H. Hartmann, M. Taglialatela, M. De Biasi, A. M. Brown, and R. H. Joho. 1992. Differences between deep pores of K^+ channels determined by an interacting pair of amino acids. *Neuron.* In press.

Lodish, H. F. 1988. Multi-spanning membrane proteins: how accurate are the models? *Trends Biochem. Sci.* 13:332–334.

MacKinnon, R. 1991. Determination of the subunit stoichiometry of a voltage-activated potassium channel. *Nature (Lond.).* 350:232–235.

MacKinnon, R., and C. Miller. 1989. Mutant potassium channels with altered binding of charybdotoxin, a pore-blocking peptide inhibitor. *Science (Wash. DC).* 245:1382–1385.

MacKinnon, R., and G. Yellen. 1990. Mutations affecting TEA blockade and ion permeation in voltage-activated K^+ channels. *Science (Wash. DC).* 250:276–279.

MacKinnon, R., L. Higginbotham, and T. Abramson. 1990. Mapping the receptor site for charybdotoxin, a pore-blocking potassium channel inhibitor. *Neuron.* 5:767–771.

Moorman, J. R., G. E. Kirsch, A. M. Brown, and R. H. Joho. 1990. Changes in sodium channel gating produced by point mutations in a cytoplasmic linker. *Science (Wash. DC).* 250:688–691.

Roux, B., and M. Karplus. 1991. Ion transport in a model gramicidin channel. Structure and thermodynamics. *Biophys. J.* 59:961–981.

Sambrook, J., E. F. Fritsch, and T. Maniatis. 1989. Molecular Cloning: A Laboratory Manual. Cold Spring Harbor Laboratory. Cold Spring Harbor, New York.

Tempel, B. L., Y. N. Jan, and L. Y. Jan. 1988. Cloning of a probable potassium channel gene from mouse brain. *Nature (Lond.).* 332:837–839.

Wilson, I. A., J. J. Skehel, and D. C. Wiley. 1981. Structure of the

haemagglutinin membrane glycoprotein of influenza virus at 3 Å resolution. *Nature (Lond.)*. 289:366–373.

Yellen, G., M. Jurman, T. Abramson, and R. MacKinnon. 1991. Mutations affecting internal TEA blockade identify the probable pore-forming region of a K^+ channel. *Science (Wash. DC)*. 251:939–942.

Yokoyama, S., K. Imoto, T. Kawamura, H. Higashida, N. Iwabe, T. Miyata, and S. Numa. 1989. Potassium channels from NG-108-15 neuroblastoma-glioma hybrid cells; primary structure and functional expression from cDNAs. *FEBS (Fed. Eur. Biochem. Soc.) Lett.* 259:37–42.

Yool, A. J., and T. L. Schwarz. 1991. Alteration of ionic selectivity of a K^+ channel by mutation of the H5 region. *Nature (Lond.)*. 349:700–704.

DISCUSSION

Session Chairman: Ron Kaback *Scribes:* Juan M. Pascual and Mingyao Liu

THADDEUS BARGIELLO: Have you examined the behavior of the reciprocal exchange chimera where the Kv3.1 channel has a Kv2.1 pore?

GLENN KIRSCH: No, we have not done that.

BARGIELLO: My concern is essentially to be able to distinguish interactions between amino acids within the pore region domain from interactions outside the domain, and the reverse chimera can give you a lot of information about it.

KIRSCH: Yes, I agree.

ALFREDO VILLARROEL: You have found a very interesting change when you mutate this L374V. I think that what is missing in your compensation experiment is to put a Leu at either position 368 or 369.

KIRSCH: At 368 we changed Val into Thr without affecting conductance. That satisfied our curiosity about the point reversion and we did not go any further with that. I guess your point is that we should find out what Leu does.

VILLARROEL: I would like to know why you changed Val to Thr at position 368.

KIRSCH: Thr is the host residue at this position, and we wanted to identify amino acid residues that specify functional differences between the host and the donor channels. We have not yet done the experiment you are asking about.

RON KABACK: Have you investigated Pro mutations in that region?

KIRSCH: We have not mutated the Pro. They are highly conserved. Our model predicts a serious disruption of the pore, but we should test this.

ROLF JOHO: Rod MacKinnon has changed one of these prolines to an alanine. They got no functional channels.

BOB GUY: In one of your earlier papers on wild-type channels you reported that internal TEA binds with the same affinity when either Val or Ile is in position 369, as long as you have Val in position 374. Now you have mutant in which a Val is present at both 369 and 374 but the TEA sensitivity is much lower than that of the two wild-type channels. Do you have any experimental evidence that these residues are involved in TEA binding?

KIRSCH: We have measured sensitivity to internal TEA in several wild-type and mutant K channels. We have found that the identity of residues at position 369 and 374 makes a difference. In the chimera, which has Val and Leu, we found low internal TEA sensitivity. When we individually revert these residues back to Kv 2.1, we find no change in internal TEA block. When we revert both of them simultaneously to Kv2.1 we restore the internal TEA sensitivity. We think that these residues are involved in specifying internal TEA binding, but we don't think they are the only residues involved.

The sequence of the wild-type Kv1.6 channel has Val in positions 374 and 369; and it also has high internal TEA sensitivity. This seems contradictory, because when we make the chimera L374V mutation, which is the same at 369 and 374 as Kv1.6 we get a different TEA sensitivity. I think their are two explanations. One reason is that we have not identified all of the determinants of the internal TEA binding site. This site is located in the internal mouth of the channel, whereas the amino acid segment we are dealing with contains mostly the external mouth, the central part, and a small part of the internal mouth. Apart from positions 374 and 369 the internal mouths of CHM and Kv2.1 are identical, whereas that of Kv1.6 may be quite different. A second reason is that we also have to consider that TEA is a open channel blocker, so its access to the binding site will depend on the gating kinetics. Mutations which decrease probability of opening will reduce TEA block. The chimera mutant L374V has low open probability and very short open times.

GUY: You are focusing only on residues that are naturally mutated in the sequence, and not working on the residues that never change normally. The potential problem is that you might be concentrating on the functionally less important residues. The fact that your mutations have effects does not necessarily mean that these are the most important residues.

KIRSCH: I agree, but wild-type K channels differ in their K/Rb conductances and position 374 may be important in specifying this difference. It is clear that we have to mutate highly conserved residues. It is also true that many of these mutants will yield nonexpressing channels. The problem is that the channel consists of four identical subunits, so every time we introduce a mutation, we are replicating it four times in the channel. There are two strategies to avoid this problem: the most direct one is to attach the subunits together with artificial linkers and make mutations in only one subunit. Alternatively, we could try rescue experiments, coexpressing wild-type and mutant subunits, and then try to distinguish the different hybrids at the single channel level.

DAVID BUSATH: Changing L374 to Val causes an increase in Rb conductance and decrease in K conductance, with little change in the selectivity ratio of Rb and K measured from bi-ionic reversal potentials. For a single ion channel, this would suggest that the affinity of a low energy site in the permeation path has increased for Rb and decreased for K. However, it is hard to imagine a binding site lined by hydrophobic side chains. (The data of Villarroel and Sakmann present the same dilemma, but at least with their data, you can invoke the Thr hydroxyl dipoles as possible cation "binders" in the wild-type). What